VEHICLE DYNAMICS

MECH 6541

Project Report

MECH 6751

For: Prof Subhash Rakheja

Submitted by-

Rahul Chug

40075138

Contents

List of Figures

Problem Statement

The cushioning of an unsprung (no suspension) service vehicle is attained through large diameter soft tires. Assuming predominantly vertical dynamics and point-contact between the tire and the ground, the vehicle can be modeled as four degrees of freedom, as shown in Figure 1.

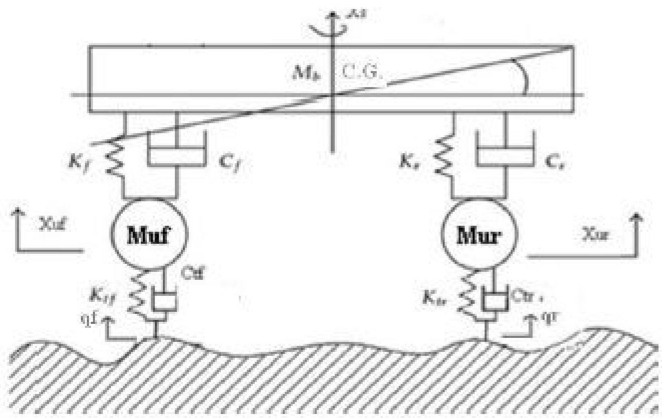

Figure 1 Four degrees of freedom suspension model

where,

Sprung Mass $M_s = 515.45$ Kg

Unsprung Front Mass $M_{uf} = 23.61$ Kg

Unsprung Rear Mass $M_{ur} = 28$ Kg

Front Suspension Stiffness $K_f = 12394$ N/m

Rear Suspension Stiffness $K_r = 14662$ N/m

Front Suspension Damping Coefficient $C_f = 692.7$ N-s/m

Rear Suspension Damping Coefficient $C_r = 817.6$ N-s/m

Tire Stiffness $K_t = 181{,}818.8$ N/m

Tire Damping Coefficient $C_t = 138$ N-s/m

Radius of Gyration R = 1.55 m

Wheelbase b = 2.5 m

Figure 2 Road bump

The vehicle is driven at a constant velocity V on a perfectly smooth road. The vehicle encounters a road bump, which can be characterized by a half-sinusoidal waveform. The height of the bump is 15 cm and its width is 1.2 m. Starting your simulations from the instant when leading edge of the bump is 10 m away from the tire-road contact point, determine the ride dynamic response of the vehicle mass.

Given constant speed of 20 Km/hr - Plot the acceleration response of the vehicle.

Plot variations in front and rear tires forces transmitted to the ground

Show that the increase in tire damping can reduce the magnitude of transmitted vibration and the dynamic forces transmitted to the pavement.

Literature review

Suspension system have always been used to study the response of rigid and multi-body systems. it was first studied by Crosby and Karnoop[1,2] for the semi active suspension system for vehicle applications. The root mean square method was also ustilized by Asami and Nishihara[3] to reduce the overall vibration transfer in the vehicle and further it was modified by Blanchard [4] to improve the ride comfort for the driver. Later on, quarter and half car model were also studied by various researchers for estimating the vehicle ride performance [5]. The study for different road profile was necessary and non- linearity had a major in comparing the results with the actual situations [6]. The theoretical results were compared with the Simulink model solution which allowed to dive into more complex and realistic suspension models [7].

Model and Assumptions

Assumptions-

1. Point contact between the tire and the road surface
2. Linear

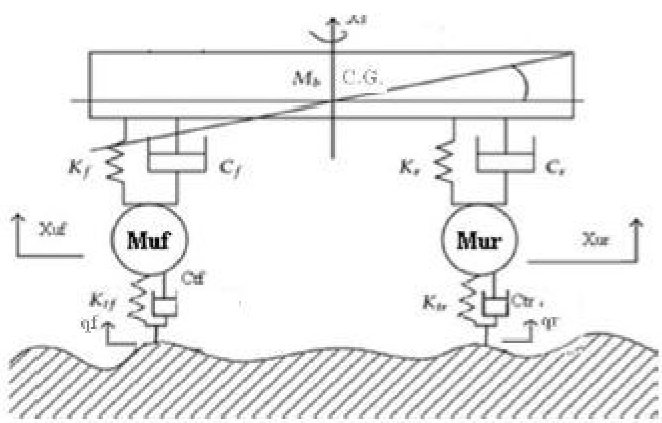

Figure 3 Free body diagram of four degrees of freedom suspension model

By Newton’s second law, the equations of motion for linear half car passive suspension model can be written as

$$M_{front} = -K_f\left(x_s - l_f\theta - x_{uf}\right)l_f + C_f(\dot{x}_s + l_f\dot{\theta} - \dot{x}_{uf})l_f$$

$$M_{rear} = -K_r(x_s + l_r\theta - x_{ur})l_r - C_r(\dot{x}_s - l_r\dot{\theta} - \dot{x}_{ur})l_r$$

$$I_y\ddot{\theta} = M_{front} + M_{rear}$$

$$M_{uf}\ddot{x}_{uf} = \left[-K_{tf}\left(x_{uf} - q\right) - C_{tf}\left(\dot{x}_{uf} - \dot{q}\right) - K_f\left(-x_s + l_f\theta + x_{uf}\right) - C_f(-\dot{x}_s + l_f\dot{\theta} + \dot{x}_{uf})\right] = 0$$

$$M_{ur}\ddot{x}_{ur} = \left[-K_{tr}(x_{ur} - q) - C_{tr}(\dot{x}_{ur} - \dot{q}) - K_r(-x_s - l_r\theta + x_{ur}) - C_r(-\dot{x}_s - l_r\dot{\theta} + \dot{x}_{ur})\right] = 0$$

Method of Analysis

The workspace table for the input variables in Simulink is shown below:

Name	Value
Cf	692.7
Cr	817.6
Ct	138
I	1238.36
Kf	12394
Kr	14662
Kt	181818.8
Lf	1.1
Lr	1.4
Ms	515.45
Muf	23.61
Mur	28
tout	[0;0.087719298245614;0.175438596...

The Simulink model for 4 degree of freedom suspension system is shown below

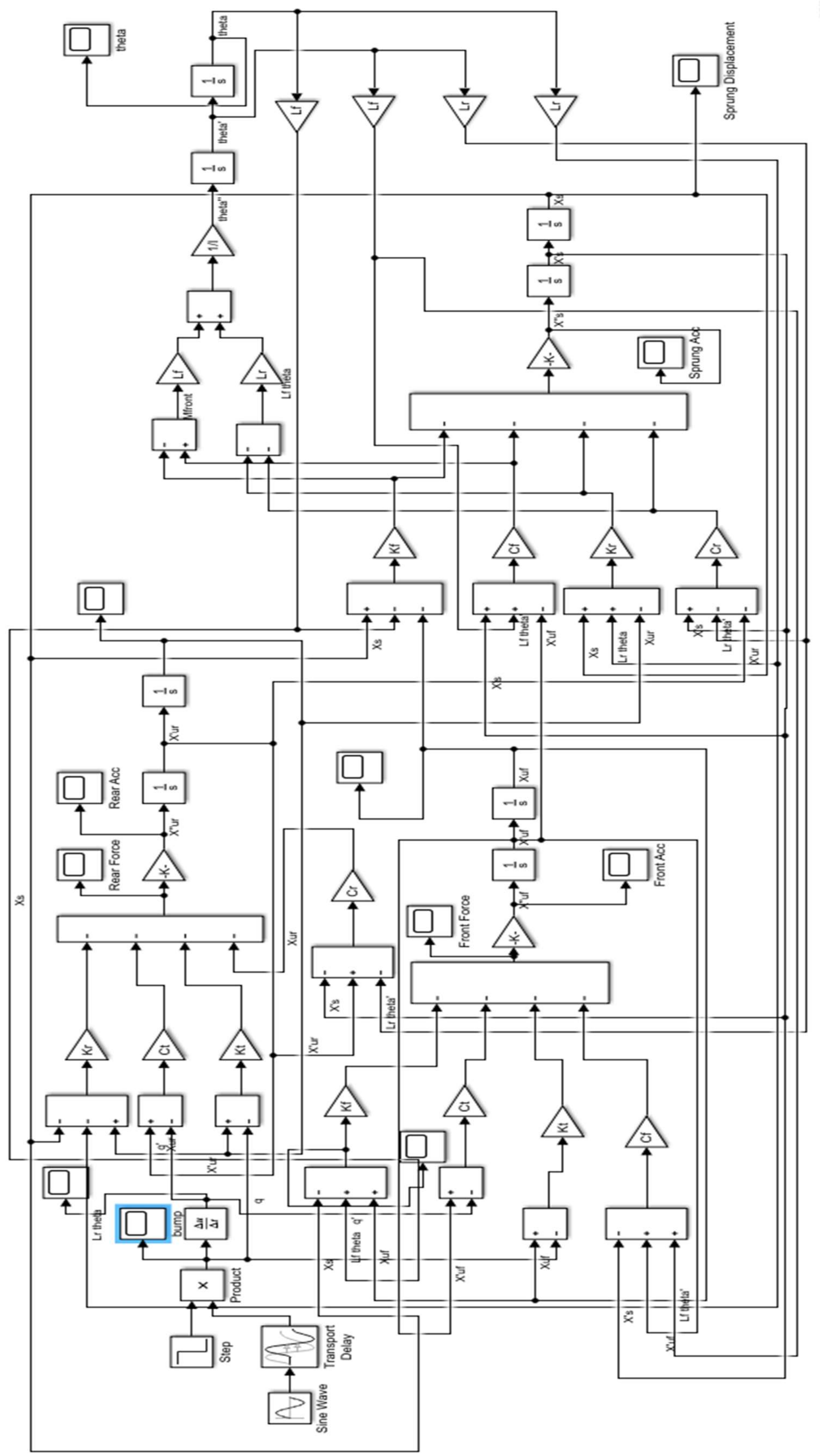
theta
Sprung Displacement
Sprung Acc
Rear Acc
Rear Force
Front Force
Front Acc
bump
Product
Step
Transport Delay
Sine Wave

Results and Discussions

The rod bump has been created with the help of step and the half sinusoidal function in the Simulink, as shown in Figure 4.

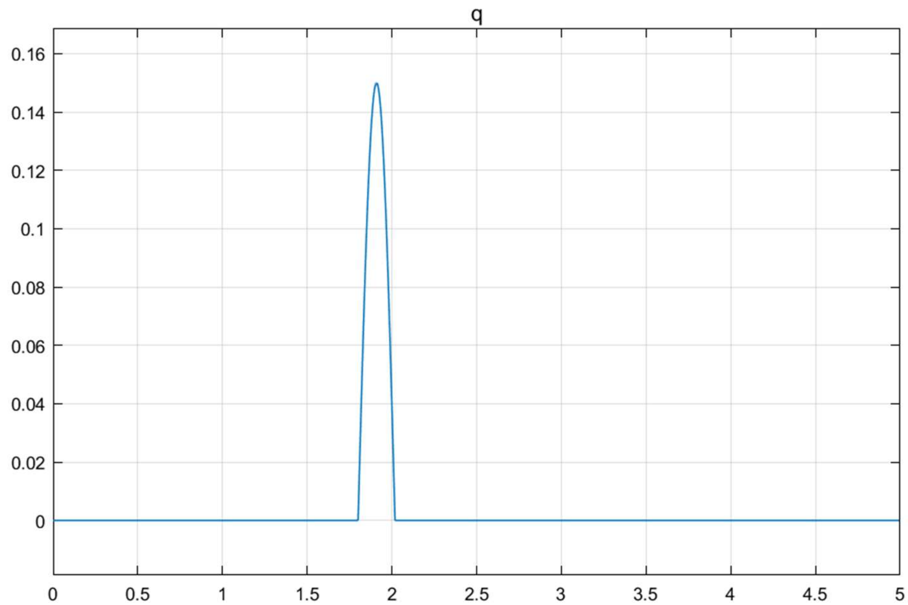

Figure 4 Generated road bump

1. Acceleration Plots

Mass acceleration plots were generated for sprung, front unsprung and rear unsprung masses. The standard damping parameter for all the developed results are C_f = 692.7 Ns/m and C_r= 817.6 Ns/m , however, to study the effect of damping capacity on the vibration of the vehicle, three different unsprung damping capacity was considered (C_f = 346.3 Ns/m and C_r= 408.8 Ns/m(half times), C_f = 692.7 Ns/m and C_r= 817.6 Ns/m and C_f = 1385.4 Ns/m and C_r= 1635.2 Ns/m(two times)) specifically for the acceleration plots.

A. Sprung Mass acceleration plot

Figure 5-7 shows the sprung mass acceleration for different damping capacity.

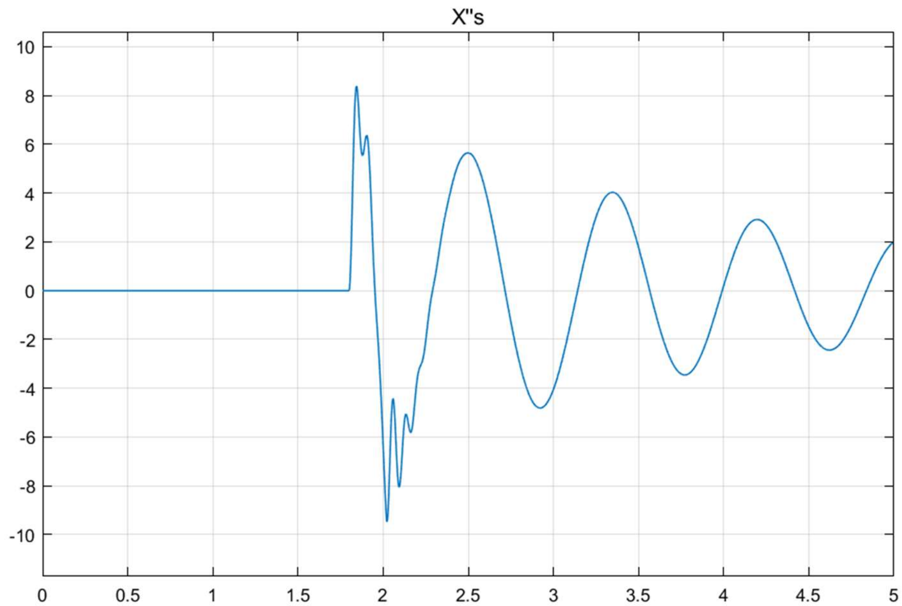

Figure 5 Sprung mass acceleration in m/s^2 for C_f = 346.3 Ns/m and C_r= 408.8 Ns/m (half times)

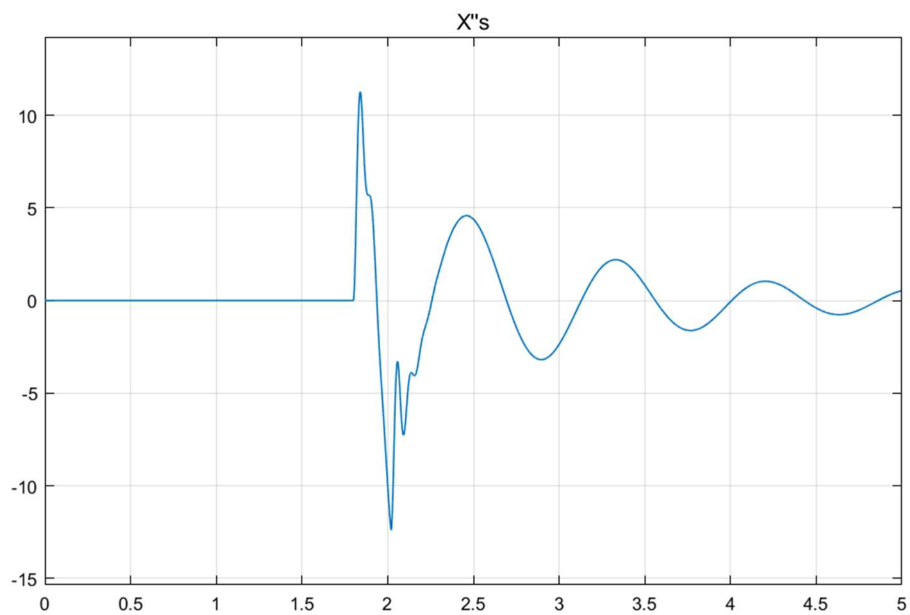

Figure 6 Sprung mass acceleration in m/s^2 for C_f = 692.7 Ns/m and C_r= 817.6 Ns/m

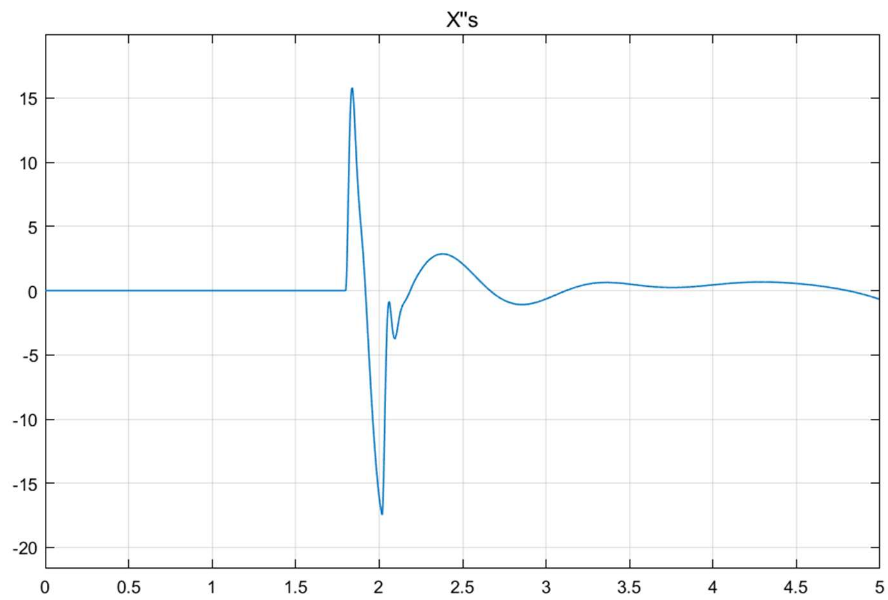

Figure 7 Sprung mass acceleration in m/s^2 for C_f = 1385.4 Ns/m and C_r= 1635.2 Ns/m (two times)

The simulation was performed for a constant velocity of 20 Km/hr (5.55 m/s) on a linear model, and it was observed that there was a significant reduction in the vibration oscillations with the increase in damping capacity as damper tends to absorb the vibrations, however, the magnitude of the vibration increases proportionally.

As can be seen in the above figures 5, for half times the standard damping, the vibration magnitude was around 8.2 m/s^2 which increased to around 12 for C_f = 692.7 Ns/m and C_r= 817.6 Ns/m and to 16 m/s^2 for 2 times the standard damping. Hence, a more comfortable ride can be possible with increased damper.

B. Front Unsprung Mass acceleration plots

Figure 8-10 shows the mass acceleration plots for front unsprung mass for different damping capacities.

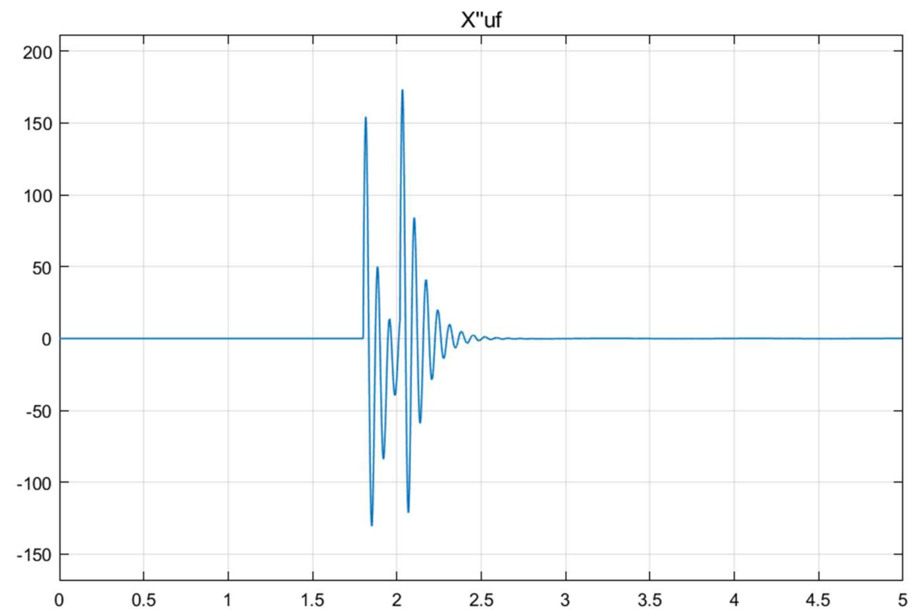

Figure 8 Unsprung mass acceleration on the front of the vehicle in m/s^2 for C_f = 346.3 Ns/m and C_r= 408.8 Ns/m (half times)

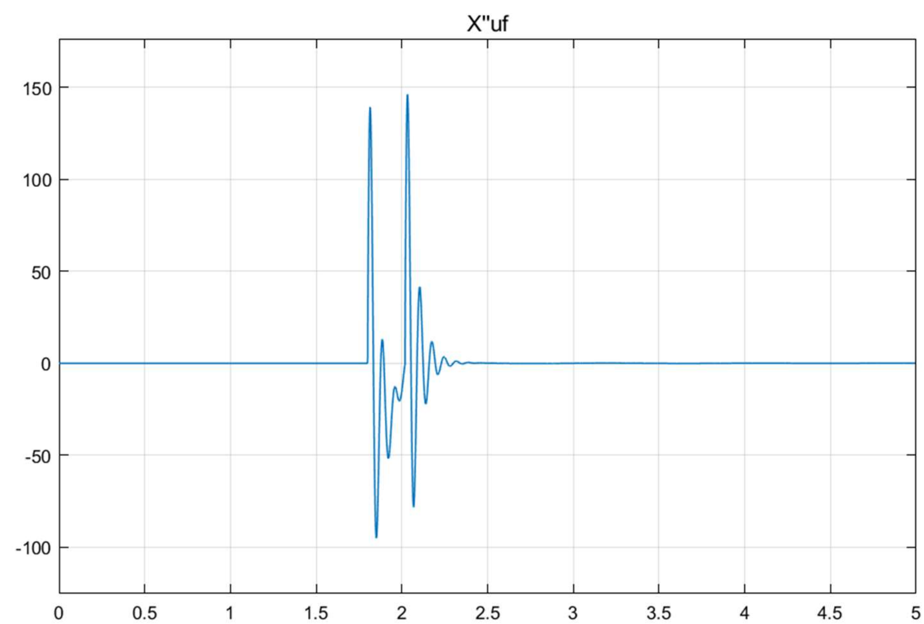

Figure 9 Unsprung mass acceleration on the front of the vehicle in m/s^2 for C_f = 692.7 Ns/m and C_r= 817.6 Ns/m

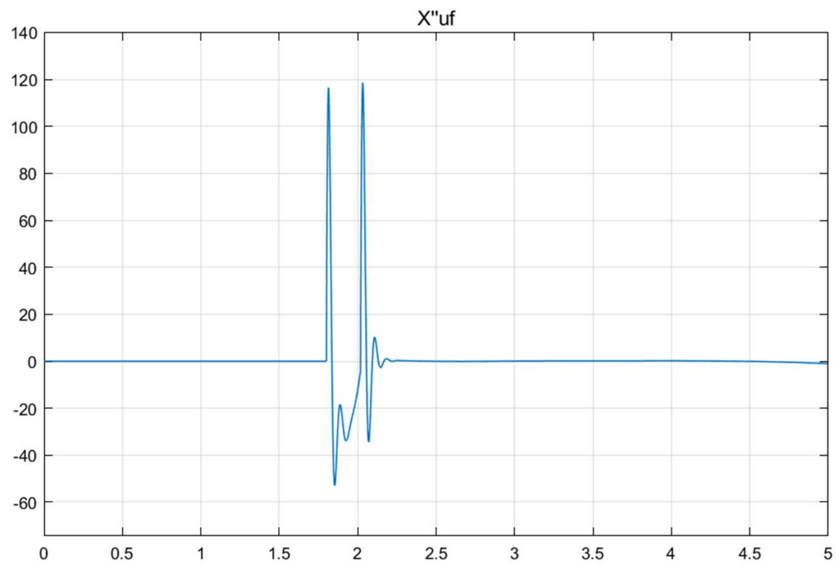

Figure 10 Unsprung mass acceleration on the front of the vehicle in m/s^2 for C_f = 1385.4 Ns/m and C_r= 1635.2 Ns/m (2 times)

As can be seen in the above plots, maximum vibration magnitude and its oscillations decreases with the increase in damping capacity since damper tends to reduce the vibration effect on the vehicle by absorbing the transmitted energy produced due to surface irregularities.

C. Rear Unsprung mass acceleration plots

Figure 11-13 shows the mass acceleration response on the rear unsprung mass for different damping capacity.

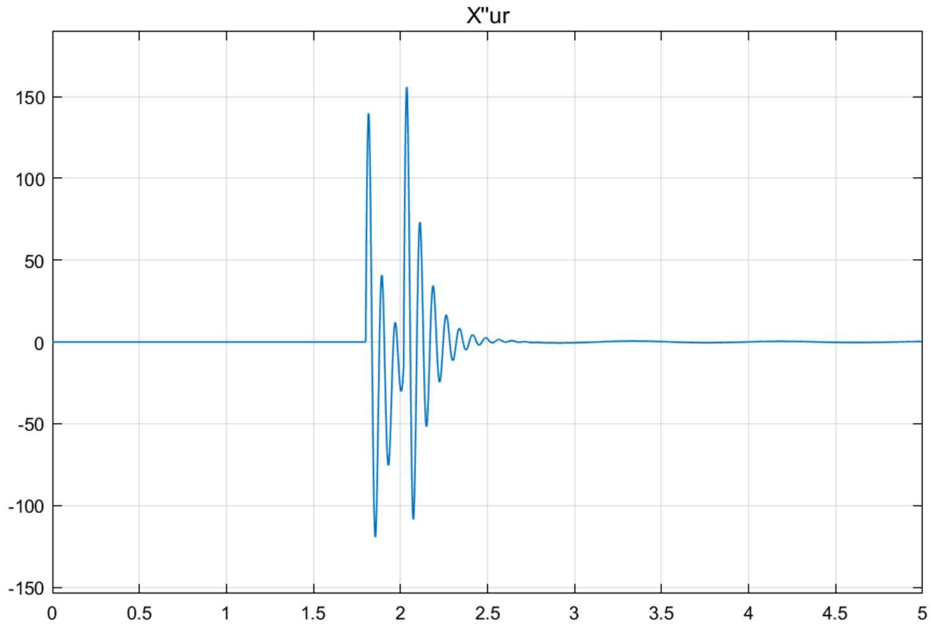

Figure 11 Unsprung mass acceleration on the rear of the vehicle in m/s^2 for C_f = 346.3 Ns/m and C_r= 408.8 Ns/m

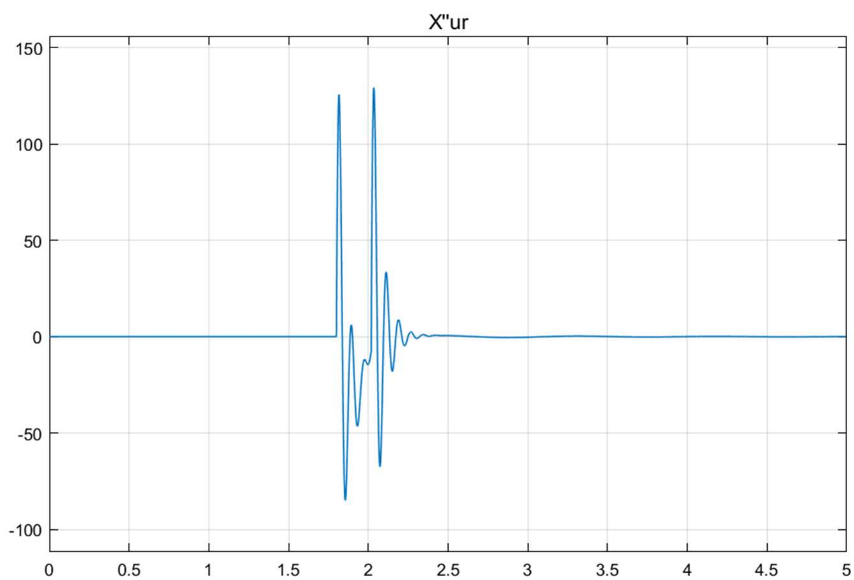

Figure 12 Unsprung mass acceleration for rear of the vehicle in m/s^2 for C_f = 692.7 Ns/m and C_r= 817.6 Ns/m

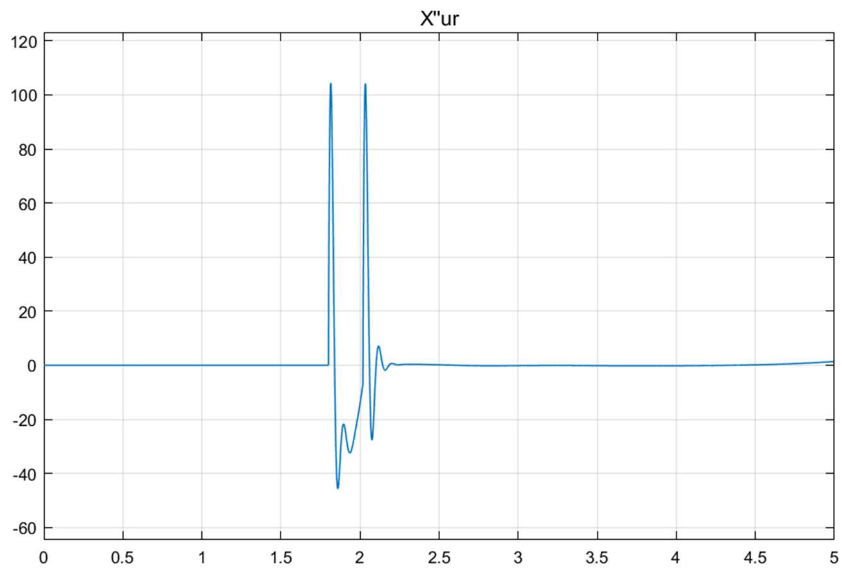

Figure 13 Unsprung mass acceleration on the rear of the vehicle in m/s^2 for C_f = 1385.4 Ns/m and C_r= 1635.2 Ns/m (2 times)

Like the behavior observed for front unsprung mass, the decrease in vibration magnitude and its oscillation with the increase in damping can be seen for rear unsprung mass too.

2. Force Plots

The force plots were simulated for the constant speed of 20 Km/r (5.55 m/s) and the damping capacity of C_f = 692.7 Ns/m and C_r= 817.6 Ns/m. All the other parameters for the simulation have been stated in the Table 1.

As can be seen in Figure 14-15, both plots show almost the same pattern for the forces, though the maximum force developed on the front axle is 3400 N, a bit lower than the rear axle force of 3500 N. Also, the force plots are consistent with the acceleration plots which were discussed earlier.

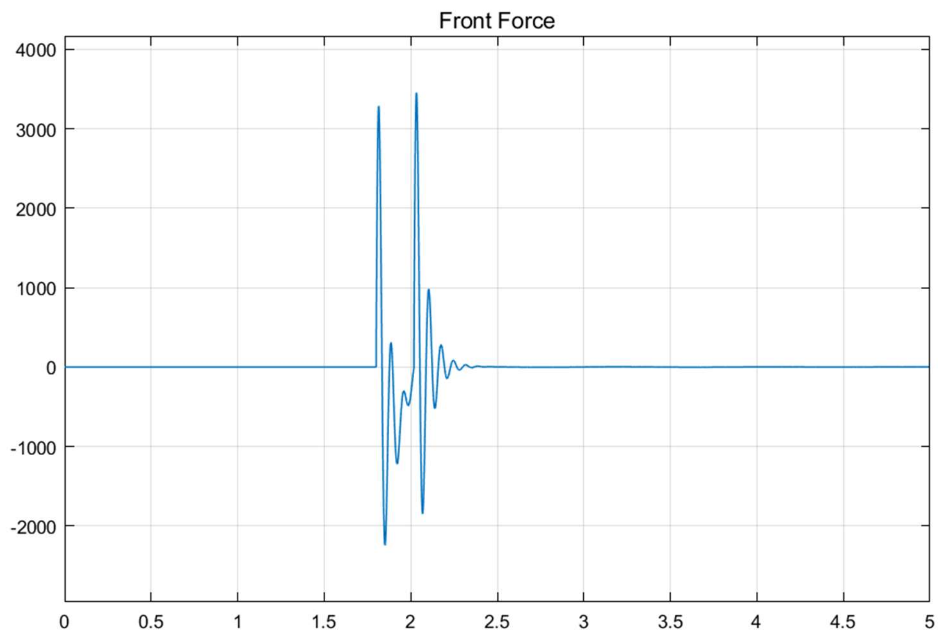

Figure 14 Force on the front of the vehicle in N

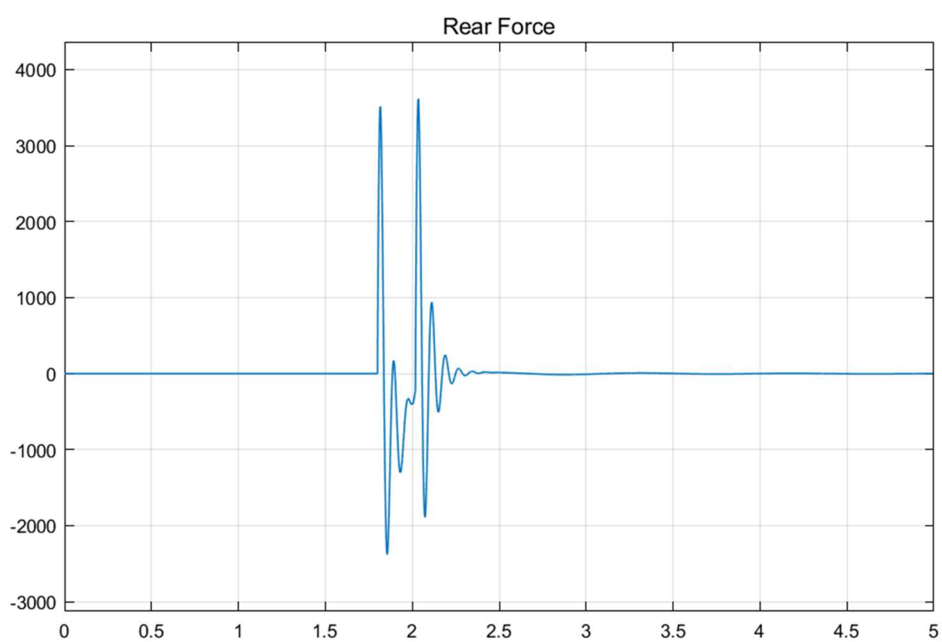

Figure 15 Force on the rear of the vehicle in N

3. Displacement Plots

The displacement plots for sprung, front unsprung and rear unsprung masses can be observed in Figures 16-18.

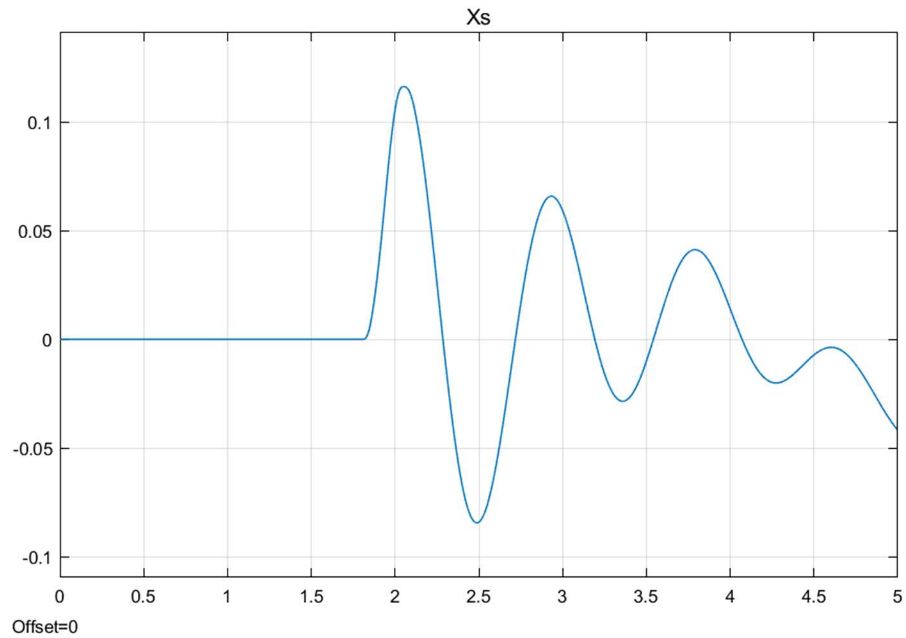

Figure 16 Sprung mass displacement of the vehicle in m

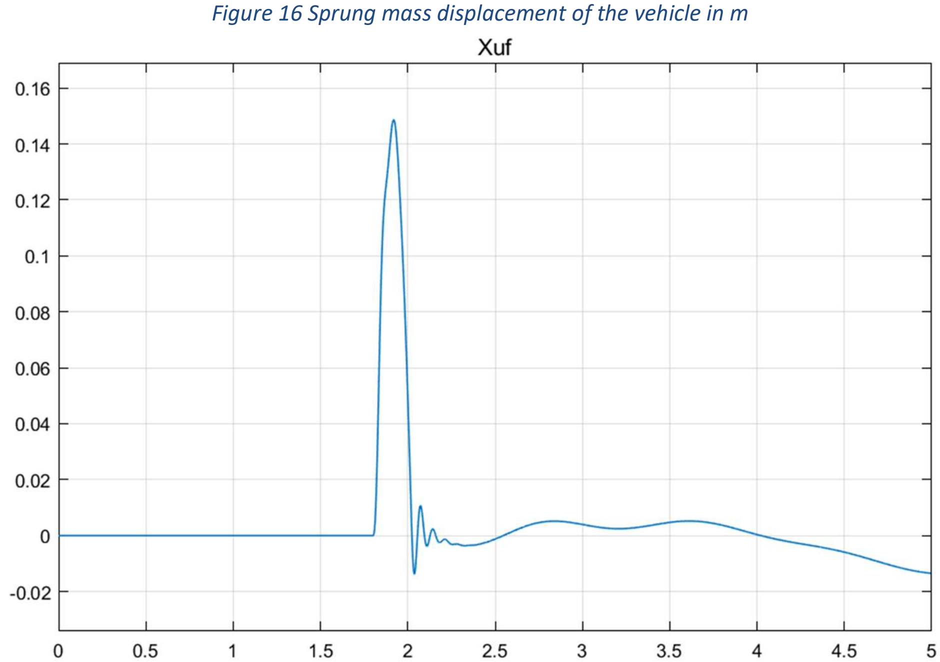

Figure 17 unsprung mass displacement on the front of the vehicle in m

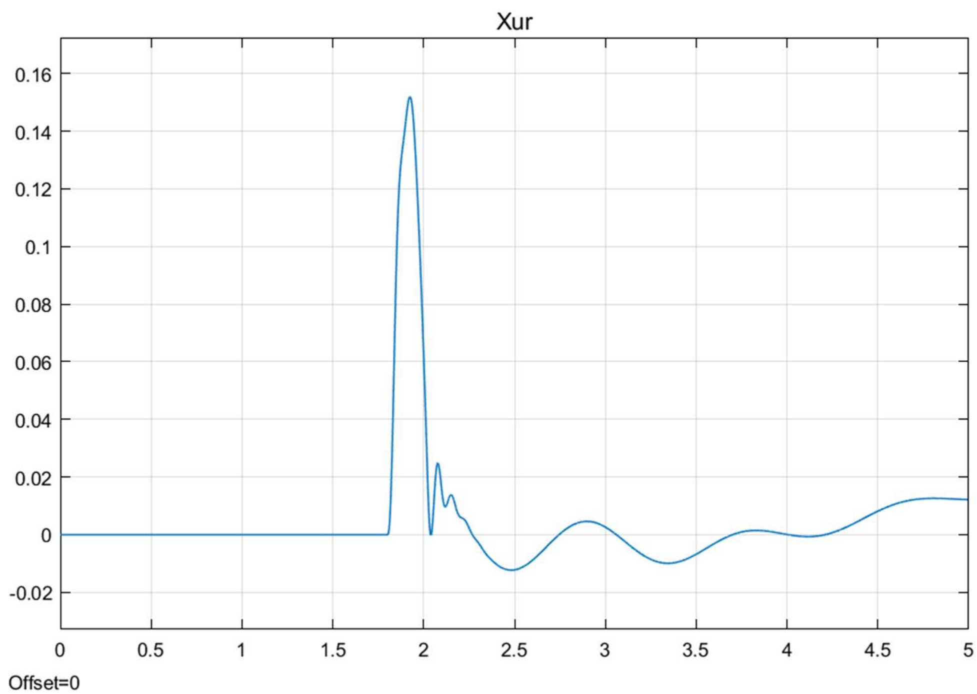

Figure 18 Unsprung mass displacement on the rear of the vehicle in m

The sprung mass displacement from Figure 16 gives a sinusoidal oscillation of 0.1 magnitude, while for unsprung masses there is a hump of 0.15 m equal to that of the bump size and then the curve is somewhat flat.

Conclusion

From the results obtained by simulation, it can be observed that by increasing the damping capacity of the tire, the vibration magnitude and the oscillations of the vehicle can be decreased for a linear passive suspension model. Further, the forces on the front and the rear axle does not show any significant difference for the given mass center, however it may be of importance for unbalanced weight vehicles. At the end, it was seen that the suspension spring and the damper could decrease the displacement magnitude of the vehicle. For future study, nonlinearity can be considered to better compare the results with the real-life situation.

References

1. M.J. Crosby and D.C. Karnopp, The Active Damper, The Shock and Vibration Bulletin 43, Naval Research Laboratory, Washington, D.C., 1973
2. D.C. Karnopp and M.J. Crosby, System for Controlling the Transmission of Energy between Spaced Members, U.S. Patent 3,807,678, April 1974
3. T. Asami and O. Nishihara, H2 Optimization to Semiactive of the Three-Element Type Dynamic Vibration Absorbers, Journal of Vibration and Acoustics 124(4) (October 2002), 583–592.
4. E.D. Blanchard, On the Control Aspects of Semiactive Suspensions for Automobile Applications, Masters Thesis, Virginia Tech. June 2003.
5. Alam, F., Faheem, A., Jazar, R., & Smith, L. V. (2010). A Study of Vehicle Ride Performance Using a Quarter Car Model and Half Car Model. *Volume 8: Dynamic Systems and Control, Parts A and B*. doi: 10.1115/imece2010-39887
6. Patole, S. & Sawant, H. (2015). Theoretical and Numerical Analysis of Half Car Vehicle Dynamic Model Subjected to Different Road Profiles with Wheelbase Delay and Nonlinear Parameters., *Int. J. of Multidisciplinary and Current research*, Vol.3, May-2015 542-46
7. Chander V, Bhanu. (2009). Modelling and Analysis of Half Car Vehicle Suspension System Using Fuzzy Logic Controller.